Eur. Phys. J. E (2012) **35**: 104
DOI 10.1140/epje/i2012-12104-0

THE EUROPEAN PHYSICAL JOURNAL E

Regular Article

Diffusion of granular rods on a rough vibrated substrate

V. Yadav[a] and A. Kudrolli[b]

Department of Physics, Clark University, Worcester, MA 01610, USA

Received 5 June 2012 and Received in final form 4 September 2012
Published online: 17 October 2012 –

Abstract. We investigate the effect of shape anisotropy and number density on the dynamics of granular rods on a substrate with experiments using a mono-layer of bead chains in a vibrated container. Statistical measures of the translational and rotational degrees of freedom indicate a dramatic slowing down of dynamics because of steric interactions at a value well below the highest packing fraction of the chains. In particular, the in-plane orientation auto-correlation function decays exponentially with time at low densities, but increasingly slowly as density is increased with a form which is not described by a simple exponential function. While the mean square displacement of the chain center of mass is observed to grow linearly at low densities, it is observed to grow increasingly slowly and non-linearly as number density is increased. Decomposing the displacements parallel and perpendicular to the long axis of the chain, we find that the ratio of diffusion in the parallel and perpendicular direction to their long axis is less than one in the dilute regime. However, as the density of the chains is increased, the ratio rapidly increases above one with a greater value for higher aspect ratios. This anisotropic behavior can be explained by considering a higher effective drag on the rods by the substrate in the perpendicular direction compared with the parallel direction, and by tube-like dynamics at higher densities.

1 Introduction

A large variety of rod-like particles exist in nature ranging from molecular polymers to bacteria and cereal grains which play a vital role in natural and industrial processes. At the smallest scales, the particles are thermally excited and their diffusion properties at equilibrium can be calculated using statistical mechanics [1]. However, it remains unclear if such an approach can describe observations in out-of-equilibrium systems such as granular materials which require constant energy input to remain active.

In fact, significant far-from-equilibrium features have been observed. For example, experiments with collection of vibrated granular rods have shown formation of dynamic vortex structures [2], and giant number fluctuations which have been described by active nematic model [3]. Details of how energy is injected can be significant, and frictional interaction with the vibrated substrate can provide preferential kicks around the axis of the rod from the point of contact towards the center of mass of the rod [4]. This effect can lead to a ratchet-like convective motion [5], and can be also exploited to fabricate self-propelled particles and study their emergent and diffusion properties [6,7].

Nonetheless, a number of recent studies with uniformly vibrated quasi-2D granular system find properties consistent with those for corresponding thermally agitated particle system. For example, experimental investigation of caging dynamics with spherical beads on a rough substrate found a number of robust features typically associated with dense molecular liquids and colloids including development of a plateau in the mean square displacement, and a Vogel-Fulcher relaxation [8]. By using a linked bead chain in a vibrated container with a rough substrate [9], preferential excitation along the axis as in the case of rigid rods appears to be reduced. This occurs because when a chain hits the vibrating plate at an angle relative to horizontal, it dissipates energy by bending and by inelastic collisions among beads in the chain reducing the kicks along the long axis. The spatial structure of such a single vibrated granular chain has been shown to be well described over a large range of lengths by a persistent self-avoided random walk model used to describe polymers [10]. Further, the diffusion of the center of mass was observed to decrease inversely with the length of the chain and consistent with Rouse dynamics.

Our goal in this paper is to discuss the diffusion of athermal rod-like particles as a function of their aspect ratio and density using chains on a vibrated substrate to minimize the preferential excitation along the axis as in rigid rods. Because the chains we use are shorter than their

[a] e-mail: vyadav@clarku.edu
[b] e-mail: akudrolli@clarku.edu

persistence length they serve as a sufficiently good approximation for rod-like particles without any subsidiary phenomenon that arise due to interaction with substrate as with rigid granular rods. We observe that the dynamics of the overall system is determined substantially by the interaction of the particles with the substrate at low concentrations, whereas the topological constraint of non-crossing of chains controls the dynamics at higher concentrations.

2 Experimental system

The chains used in the experiments are composed of beads with diameter $d = 3.2\,\text{mm}$ which are linked with a loose link whose length can vary from 0 to 1.1 mm. We use chains with bead number $n = 2$, 3 and 5 to vary the length L of the rod. The aspect ratio $A_r = L/d$ of the chains are accordingly found to be on average 2.34, 3.78 and 6.41. Because each link can bend so that neighboring bonds between the beads in the chain can be between $\pi/4$ and $-\pi/4$, we choose a small number of beads to ensure that the length of the chain is smaller than its persistence length of $\approx 10d$ [10]. To test our assumption on approximation of granular chain as rods we calculated the probability distribution of fluctuation of beads about the line of best fit. We observed that for longest chain (*i.e.* 5 beads) in dilute regime the fluctuation was less than 1 bead diameter in 87% of the observations. In concentrated regime, 91% of the cases had fluctuation that was less than 1 bead diameter. Smaller chains will have even smaller fluctuation due to reduced number of links, and therefore we assume that all the chain lengths used in this study can be approximated as granular rods. The experimental setup consists of a circular container with diameter $d_{\text{base}} = 28.5\,\text{cm}$ ($89d$) mounted on an electromagnetic shaker. A layer of 1 mm steel beads were glued to the surface of plate to make it rough. This ensures random kicks with components in the lateral direction when the chain collides with the substrate and results in greater in-plane dynamics. The system is then vibrated sinusoidally at a peak acceleration of $3g$, where $g = 9.8\,\text{m s}^{-2}$. The acceleration provides sufficient driving force not only in the vertical direction to move the chain over the roughness scale, but does not allow them to hop over each other. While a rod can have three translational and three rotational degrees of freedom, one degree of freedom each is suppressed as the rods do not travel significantly off the substrate, and do not flip in a vertical plane.

We vary the number of chains in the system to change the area fraction ϕ which is defined as

$$\phi = nmd^2/d_{\text{base}}^2, \tag{1}$$

where n is the number of beads in each chain and m is the number of chains in the system. Accordingly, the area fraction ϕ^* corresponding to the transition from the dilute to the semi-dilute density is given by n/A_r^2, and the concentrated regime corresponds to above $\phi_c = \pi n/4A_r$. The corresponding values for the chains used in our experiments are shown in table 1. While the chains used

Table 1. The area fractions $\phi*$ and ϕ_c corresponding to the transition from the dilute to the semi-dilute and to the concentrated regimes.

n	$\phi*$	ϕ_c
2	0.36	0.67
3	0.21	0.62
5	0.12	0.61

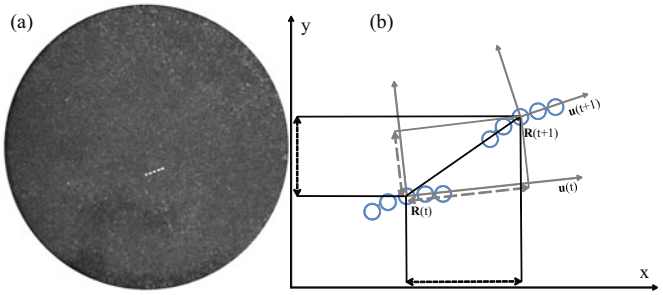

Fig. 1. (a) An image of a chain with 5 beads in the circular container with a rough horizontal substrate. (b) A schematic diagram denoting the position vector of the center of mass $\boldsymbol{R}(t)$ and $\boldsymbol{R}(t+1)$ at time t and $t+1$, respectively, along with the corresponding orientation vector $\mathbf{u}(t)$ and $\mathbf{u}(t+1)$. Solid black and gray frames depict lab and body frame of reference, respectively. The components of the displacements in the lab and body frame are denoted by dashed lines of same color as the frame.

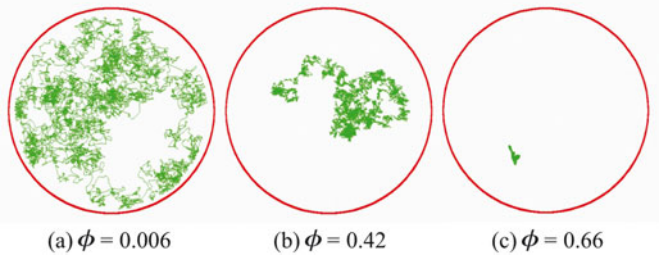

Fig. 2. Sample trajectory of a chain with 5 beads corresponding to (a) dilute regime $\phi = 0.006$ over time interval $\Delta t = 1200\,\text{s}$, (b) semi-dilute regime $\phi = 0.42$ over $\Delta t = 1200\,\text{s}$, and (c) concentrated regime $\phi = 0.67$ over $\Delta t = 3600\,\text{s}$. The diffusion of the chain slows down as ϕ increases, and the observation period was changed accordingly.

are identical and colored black, a single chrome plated but otherwise similar chain is used as a tracer to measure position over long periods of time using a mega-pixel digital camera. A typical image is shown in fig. 1 along with a schematic representing the laboratory reference frame and the body reference frame of the rod. Because smaller chains have faster dynamics compared to larger chains [10], chains with 2 beads were tracked at 20 frames per second (fps) and the chains with 3 and 5 beads were tracked at 10 fps. The images were then used to calculate position and orientation of rods in the laboratory reference frame in the horizontal plane. Typical reconstructed trajectories corresponding to various ϕ are shown in fig. 2.

The rods diffuse over the entire container at low density but appear confined at the highest density. Because of the tracer technique used here we confine our discussion to dynamics. Spontaneous pattern formation has been discussed using rigid granular rods by others [11].

3 Rotational diffusion

We first examine the dynamics using the orientation of the chain in the horizontal plane. We obtain the orientation of the chain by fitting the bead positions with a line which minimizes its radius of gyration. If $\boldsymbol{u}(t)$ is the unit orientation vector of the chain at time t, then we can evaluate the orientation auto-correlation function $C_D(t) = \langle \boldsymbol{u}(t) \cdot \boldsymbol{u}(t + t_0) \rangle$. Figure 3(a-c) shows the decay of $C_D(t)$ for chains with $n = 2$, 3, and 5 at various area fraction. A star denotes the area fraction ϕ^*, which corresponds to transition from dilute to semi-dilute regime. The upper range of ϕ investigated in our experiments is determined by the value where the chains are no longer confined in a single layer but start to form double layers, and only the $\phi = 0.66$ for the 5 bead chain falls in the concentrated regime. As expected, we observe that the decay is rapid at low densities but becomes slower as the density is increased due to interactions with other particles. Except for the data in the concentrated regime, $C_D(t)$ is observed to approach $4/\pi^2$, which corresponds to uncorrelated orientations in case of rods.

In fig. 4, we plot $C_D(t)$ after subtracting $4/\pi^2$ *versus* time to examine the rapid initial decay. In the dilute regime, we find that $C_D(t)$ decays as an exponential from which a single relaxation time scale can be extracted. However, this trend is not observed in the semi-dilute regime where chains interact more frequently and perhaps multiple time scales may be in play. This lack of single relaxation time scale becomes an issue when we try to define a rotational diffusion coefficient from $C_D(t)$ at high concentrations. Therefore, we define a rotational diffusion coefficient D_r to be inverse of a characteristic decay time in which $C_D(t)$ decays to half of its initial value. In fig. 5, we plot D_r as a function of ϕ for various A_r. For the same ϕ, we find that D_r of a chain with larger aspect ratio is smaller than that of a chain with smaller aspect ratio. This is attributed to the fact that the rods with larger A_r will have a larger probability of colliding and hindering the rotational motion of nearby rods at fixed ϕ, thus reducing the overall D_r.

Using a tube model, Doi and Edwards calculated [1] that the rotational diffusion coefficient in the semi-dilute regime, D_r, and dilute regime, D_{r0}, in 3D are related by

$$D_r = \beta D_{r0} (\nu L^3)^{-2}, \qquad (2)$$

where ν is the concentration of rod-like particles in three dimensions, and β is a constant. However, when the measured D_r is scaled with D_{r0} and plotted against reduced concentration in 2D (*i.e.* νL^2), a collapse of reduced rotational diffusion coefficients for chains of different lengths

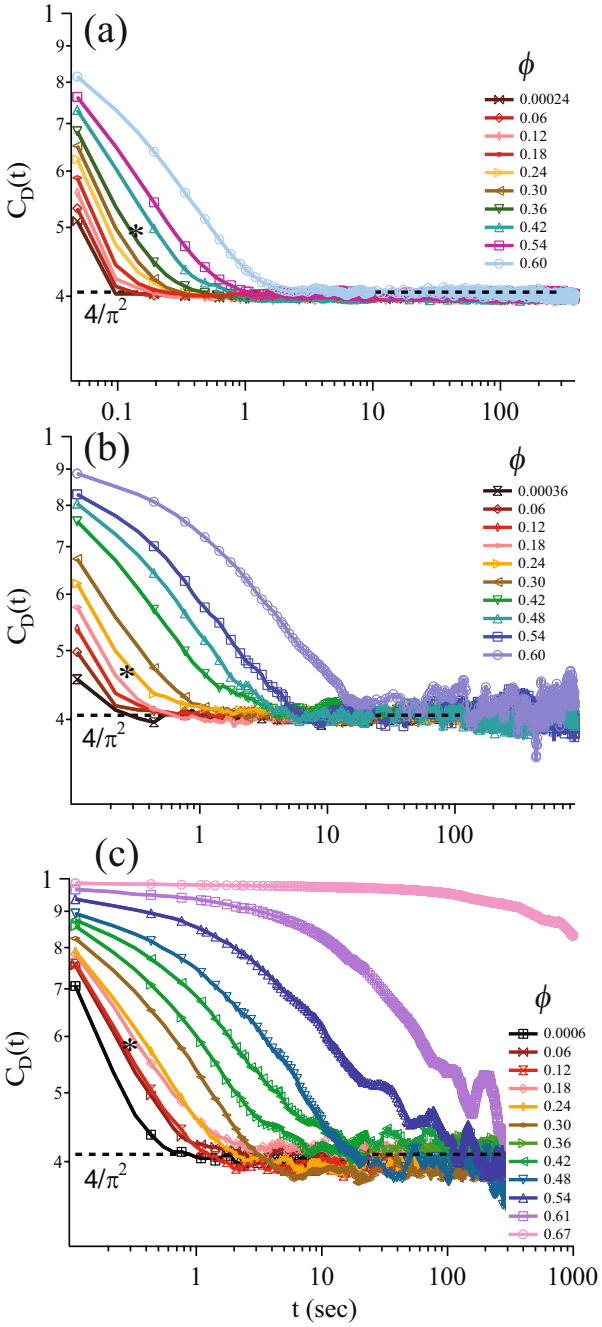

Fig. 3. The decay of the orientation auto-correlation function for chains with (a) $n = 2$, (b) $n = 3$, and (c) $n = 5$. The star indicates the area fraction where system goes from dilute to concentrated regime, with $\phi^* = 0.37$, 0.21 and 0.12 for rods with $n = 2$, 3 and 5, respectively.

(which is linearly proportional to the rod mass) is not observed (see fig. 6). This can be explained if we take into account the rotation of rods along their long axis. In 3D, a rod of length L disengages from the constraints of a tube of radius a by moving a distance of length $L/2$ along its long axis. Over the same time it rotates by an angle of order a/L. In 2D, when a rod meets a constraint posed by a tube it rotates about the point of contact due to the ro-

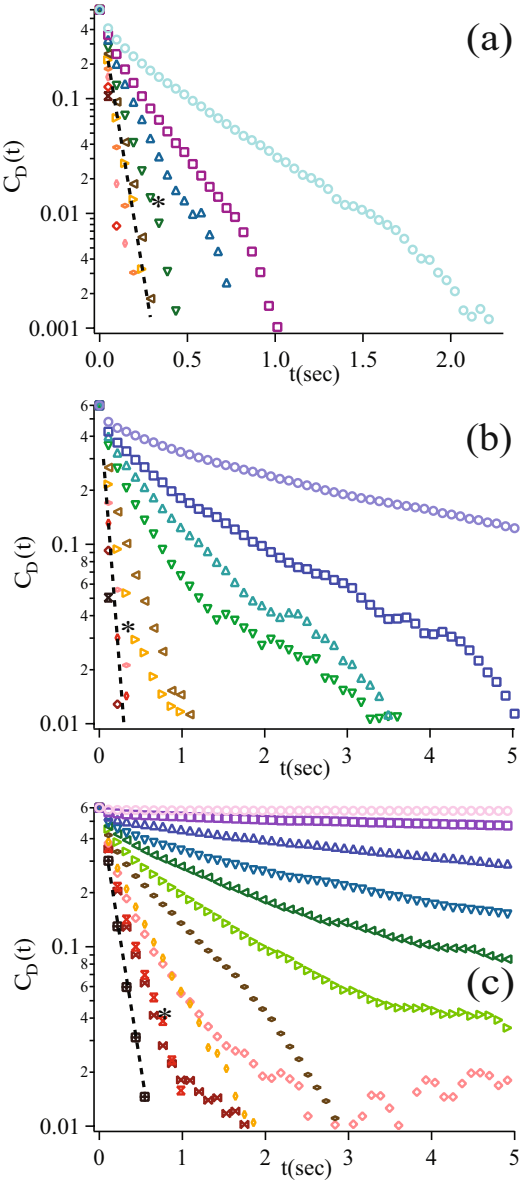

Fig. 4. Semi-log plot of $C_D(t)$ for chains with (a) $n = 2$, (b) $n = 3$ beads, (c) $n = 5$. In the dilute regime, the decay can be described by an exponential fit, this is not in the semi-dilute regime where the decay curve may have multiple time scales.

tational inertia of rod along its long axis hence decreasing the overall angle traveled by the rod. Because the angle by which a rod rotates is presumably inversely proportional to its moment of inertia and hence to its mass, eq. (2) can be modified as

$$D_r = \beta D_{r0}(1/\nu L^2 - K/n)^{\alpha}. \qquad (3)$$

We observe that for $K = 0.6$, all the normalized diffusion curves collapse on to each other with an exponent of $\alpha = 2.0$ in semi-dilute regime. Fitting the collapsed data with a single parameter function (eq. (3)) in β, we find $\beta \approx 13.68$ which is greater than what is assumed by Doi and Edwards who consider it to be of order unity. However, it is noteworthy that the observed α is smaller compared

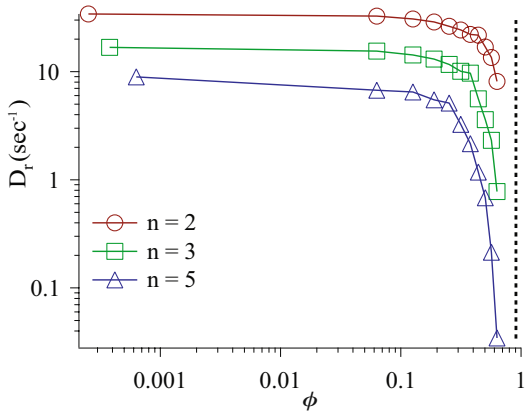

Fig. 5. Decay of the rotational diffusion coefficient D_r as a function of area fraction for chains of different lengths. The dashed vertical line represents ϕ corresponding to the densest possible packing of the bead chain in our system, *i.e.* $\pi/2\sqrt{3} \approx 0.91$.

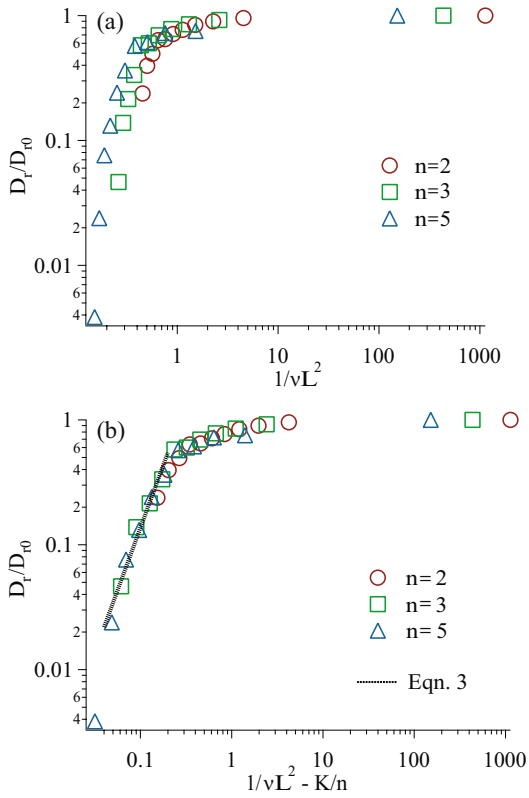

Fig. 6. (a) The normalized rotational diffusion coefficient as a function of concentration. Curves for chains of different A_r do not converge on a single line as observed in case of thermal rods. (b) The normalized rotational diffusion coefficient plotted against modified concentration. The curves for different athermal chains fall on the same master curve with the same exponent as predicted for thermal rods.

to values reported in 3D [1,12]. We note that we have changed our control parameter from volume fraction, ϕ to reduced concentration, *i.e.* νL^2 to avoid introducing an extra dependence on the number of beads in eq. (2).

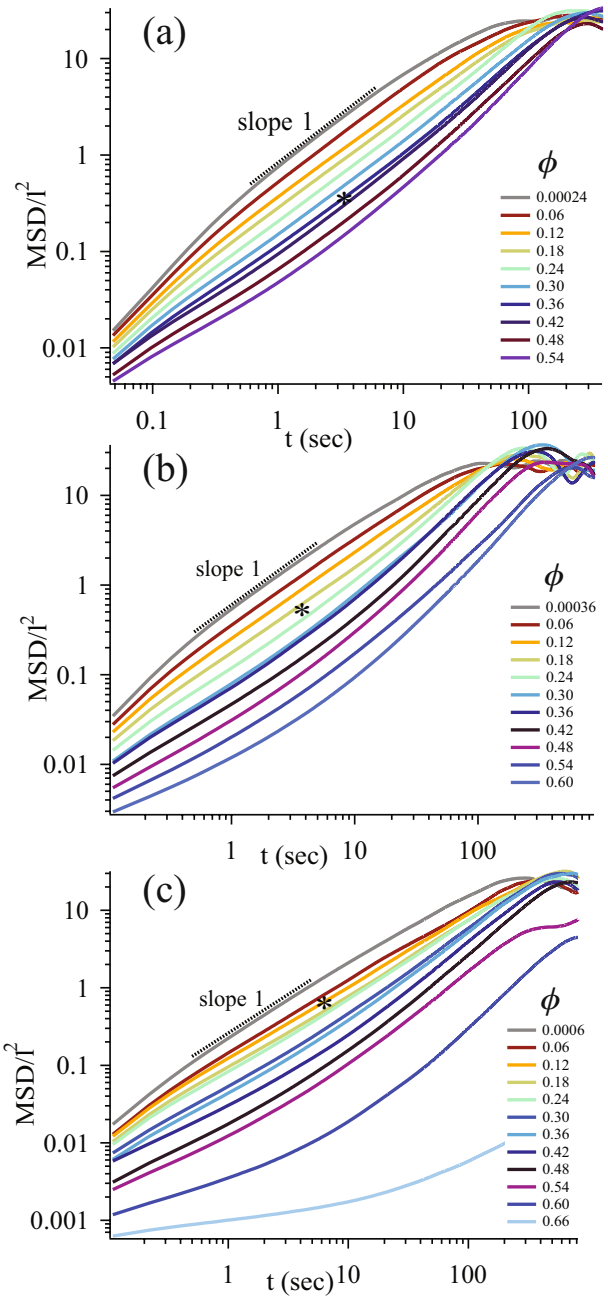

Fig. 7. The mean square displacement (MSD) as a function of time for chains with (a) $n = 2$, (b) $n = 3$, and (c) $n = 5$. The star indicates the area fraction where system goes from dilute to concentrated regime (for values refer to fig. 3).

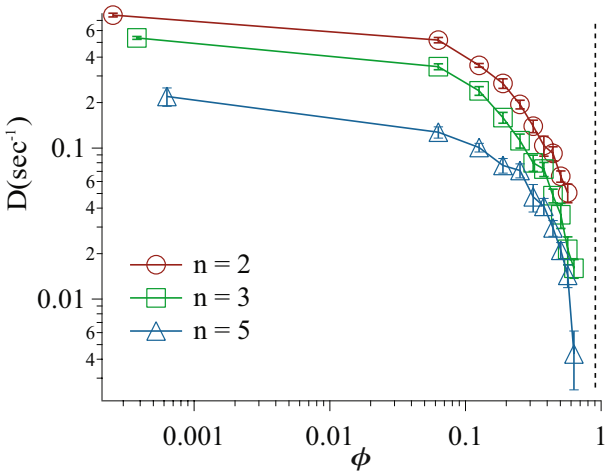

Fig. 8. Decay of the total diffusion coefficient as a function of area fraction for chains of different lengths. The dashed black line represents ϕ corresponding to the densest possible packing in our system, *i.e.* 0.91.

4 Translational diffusion

4.1 Translational diffusion in lab frame

We next turn to the analysis of the mean square displacement (MSD) of the rods in the laboratory frame of reference. If $\boldsymbol{R}(t')$ is the position of center of mass of tracer chain at time t', then MSD over a time t is defined by $\langle \Delta \boldsymbol{R}^2(t) \rangle = \langle (\boldsymbol{R}(t + t_0) - \boldsymbol{R}(t_0))^2 \rangle$. In fig. 7, we plot $\langle \Delta \boldsymbol{R}^2(t) \rangle$ against time for various area fractions for chains of different length. Here, the vertical axis is scaled over a distance $l = R_{\text{base}}/5$ over which a chain travels in the dilute regime before becoming diffusive. We observe at short time scales that the motion is super-diffusive, which is a signature of transition from ballistic to diffusive regime. (By performing a limited set of experiments with a faster than 1000 frame rate camera, we were able to verify that a ballistic regime indeed exists over time scales shorter than 20 ms.) At intermediate time scales, the motion of chains is diffusive in the dilute regime but becomes more and more sub-diffusive as the area fraction increases. The MSD plots also shows two distinct time scales at higher concentrations. Here, the slow mode is due to caging of a chain by its neighbors, and the fast decay mode is due to rapid motion after cage breaking. At long time scales, we observe that MSD starts saturating at a length scale corresponding to the size of the container.

As with rotational diffusion, it is difficult to determine the translational diffusion constant from a linear fit of $\langle \Delta \boldsymbol{R}^2(t) \rangle$. Therefore, we deduce a translational diffusion coefficient D by defining it as the inverse of a characteristic time scale over which a particle diffuses by a distance of l. The translational diffusion coefficient *versus* ϕ for chains of different lengths is plotted in fig. 8. We observe a systematic decrease in D with an increase in the number of beads in the chain at low densities. In a previous work by Safford *et al.* [10] it has been shown that the chains show Rouse dynamics, *i.e.* D decays as $1/n$ in the dilute regime which is consistent with the observations shown here. Further it can be noted that the rapid decrease of diffusion occurs in the semi-dilute regime, and the chains appear caged well before the highest packing fraction 0.91 possible for the chain system. In the case of spheres, Reis *et al.* [8] observed that the particles appear caged above $\phi \sim 0.72$ with a similar vibration system and close to the crystallization transition. In our experiments with non-spherical particles, caging appears to occur at a lower value, and is at least as low as 0.66 in the case of $n = 5$.

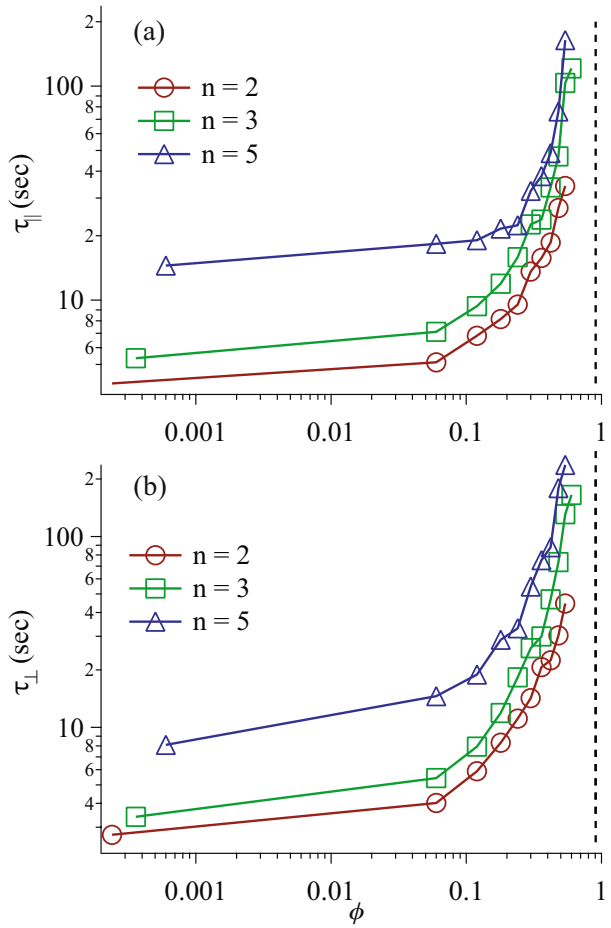

Fig. 9. Variation of mean time required to diffuse through a distance l in a direction (a) parallel and (b) perpendicular to rod, respectively, as a function of area fraction. The dashed black line represents ϕ corresponding to the densest possible packing in our system, *i.e.* 0.91.

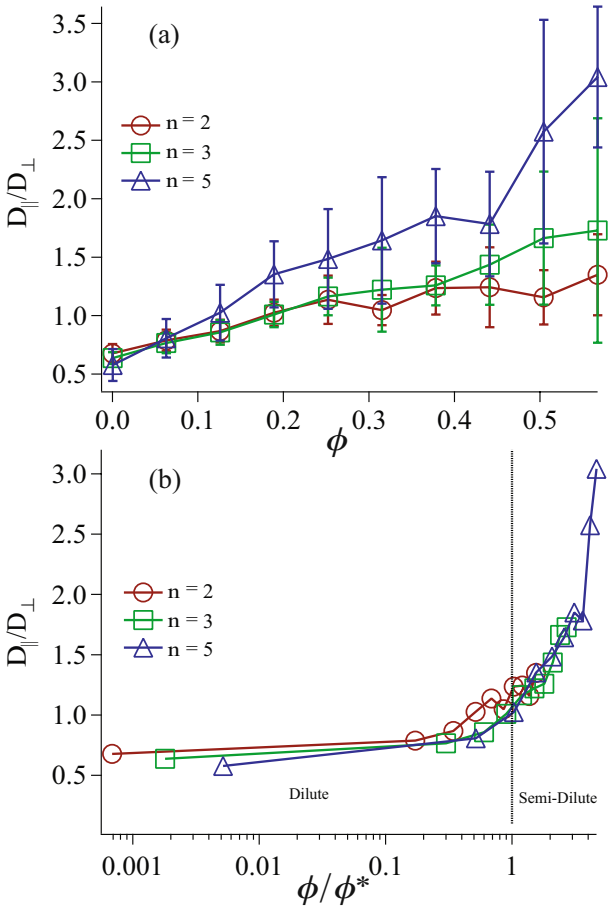

Fig. 10. (a) Ratio of diffusion coefficient in parallel and perpendicular direction ($D_{\parallel}/D_{\perp}$) is plotted against area fraction for rods of different lengths. (b) $D_{\parallel}/D_{\perp}$ is plotted against scaled area fraction. It is clearly observed that $D_{\parallel}$ is less than $D_{\perp}$ in the dilute regime.

4.2 Translational diffusion in body frame

Any anisotropy of diffusion is not directly evident in laboratory frame due to the rotation of the rod in the horizontal plane. Therefore, we decompose the displacement of the chain in a body frame attached to the center of mass of the chain with an axis oriented along the long axis of the chain which minimizes its radius of gyration and the other axis oriented perpendicular to it. Again, we can define a diffusion constant in a given direction to be the inverse of a characteristic time that the particle takes to diffuse by a distance of l in that direction. In fig. 9, we plot the variation of characteristic time scales in parallel ($\tau_{\parallel}$) and perpendicular ($\tau_{\perp}$) directions for chains of various aspect ratios as a function of their area fraction. Overall, we find similar trends for $\tau_{\parallel}$ and $\tau_{\perp}$ with higher time scales for higher aspect ratios. This can be attributed to more frequent collisions among beads in chain along its length. Further it may be noted that the time scales for parallel and perpendicular components diverge together and over apparently similar ϕ as the net diffusion.

To understand the differences, we obtain the ratio $D_{\parallel}/D_{\perp} = \tau_{\perp}/\tau_{\parallel}$ in the dilute and semi-dilute regime and plot it in fig. 10(a) as a function of ϕ, and as a function of ϕ scaled with corresponding ϕ^* in fig. 10(b). We find that the data organizes such that the $D_{\parallel}/D_{\perp}$ in the dilute regime is less than one for all chains, and increases above one in the semi-dilute regime. In case of a randomly excited rod moving in 2D with slip boundary conditions, the ratio should be equal to one if the dissipation is independent of orientation with respect to its velocity. However, if the dissipation depends on orientation then the ratio can be non-zero depending on the aspect ratio even in case of thermal excitation [13]. Because we have used semi-flexible chains in our experiments which do not get preferential kicks along their axis as in case of rigid rods on a frictional substrate [4], the relatively greater diffusion in the perpendicular direction must be a result of lower dissipation compared to that in the parallel direction at low densities. We believe this lower dissipation occurs because of rolling of rods, which increases the diffusion in perpendicular direction. Close to ϕ^* this rolling is arrested and we observe that the ratio $D_{\parallel}/D_{\perp}$ tends to one for rods of all aspect ratios. In the semi-dilute regime, chain interactions become important, and the system starts showing

tube-like dynamics as we have inferred from the rotational diffusion in the previous section. In this model, a rod-like particle cannot move as easily in the perpendicular direction compared with the parallel direction because of the enhanced probability of encountering another particle. Accordingly a rod-like particle is observed to diffuse by rotating by an angle $1/A_r$ as it moves. Thus, $D_\parallel/D_\perp$ can be expected to become of order A_r as density is increased in the semi-dilute regime before the rods get caged. The increasing $D_\parallel/D_\perp$ with A_r shown in fig. 10 are consistent with this trend.

5 Conclusions

Using linked chains on a vibrated substrate, we have studied the diffusion of granular rod in two dimensions and find significant effects due to their aspect ratio and density. Multiple time scales in rotational as well the translational diffusion degree of freedom are observed in the semi-dilute regime. We observe that rolling of rods can have significant effect on their dynamics due to the low moment of inertia of the rods about their long axis and frictional substrate. Due to presence of rolling, D_r was estimated to be modified to a smaller value in semi-dilute regime. Further, the diffusion coefficient in perpendicular direction was observed to be higher than the diffusion coefficient in parallel direction in the dilute regime. In the semi-dilute regime, chain interactions become important and the diffusion along the parallel direction is to be greater than the perpendicular direction given by a factor which increases with aspect ratio, consistent with tube-like dynamics. Finally, chains are observed to become caged at a lower area fraction than spheres moving on a vibrated substrate.

We thank Thomas Garnier for help with preliminary experiments. This work was supported by the National Science Foundation under NSF Grant No. CBET-0853943 and by the Jan and Larry Landry Chair Fund.

References

1. M. Doi, S.F. Edwards, *The Theory of Polymer Dynamics* (Clarendon Press, Oxford, 1999).
2. Daniel L. Blair, T. Neicu, Arshad Kudrolli, Phys. Rev. E **67**, 031303 (2003).
3. Vijay Narayan, S. Ramaswamy, Narayanan Menon, Science **317**, 107 (2007).
4. Dmitri Volfson, Arshad Kudrolli, Lev S. Tsimring, Phys. Rev. E **70**, 051312 (2004).
5. S. Dorbolo, D. Volfson, L. Tsimiring, A. Kudrolli, Phys. Rev. Lett. **95**, 044101 (2005).
6. A. Kudrolli, G. Lumay, D. Volfson, L. Tsimiring, Phys. Rev. Lett. **100**, 058001 (2008).
7. A. Kudrolli, Phys. Rev. Lett. **104**, 088001 (2010).
8. P.M. Reis, R.A. Ingale, M.D. Shattuck, Phys. Rev. Lett. **98**, 188301 (2007).
9. E. Ben-Naim, Z.A. Daya, P. Vorobieff, R.E. Ecke, Phys. Rev. Lett. **86**, 1414 (2001).
10. K. Safford, Y. Kantor, M. Kardar, A. Kudrolli, Phys. Rev. E **79**, 061304 (2009).
11. Jennifer Galanis, Daniel Harries, Dan L. Sackett, Wolfgang Losert, Ralph Nossal, Phys. Rev. Lett. **96**, 028002 (2006).
12. M. Doi, I. Yamamoto, F. Kano, J. Phys. Soc. Jpn. **53**, 3000 (1984).
13. Y. Han, A.M. Alsayed, M. Nobili, J. Zhang, T.C. Lubensky, A.G. Yodh, Science **314**, 626 (2006).